Fungi-derived pigments as sustainable organic (opto)electronic materials

Robert Harrison[a], Alexander Quinn[a], Genevieve Weber[b], Brian Johnson[a], Jeremy Rath[a], Vincent Remcho[c], Sara Robinson[d], and Oksana Ostroverkhova[a]

[a]Oregon State University, Dept. of Physics, Corvallis, OR 97331, USA
[b]Oregon State University, Dept. of Botany & Plant Pathology, Corvallis, OR 97331, USA
[c]Oregon State University, Dept. of Chemistry, Corvallis, OR 97331, USA
[d]Oregon State University, Dept. of Wood Science & Engineering, Corvallis, OR 97331, USA

ABSTRACT

We present photophysical and optoelectronic properties of xylindein and optical properties of two other fungi-derived organic pigments. Photophysics of these materials is determined by the interplay of inter- and intramolecular hydrogen bonding, which was systematically explored using absorption and photoluminescence spectroscopy of xylindein in various solutions, pH buffers, and in the solid state. Amorphous xylindein films yielded a lower bound on the charge carrier mobility of 0.2-0.5 $cm^2/(V \cdot s)$ and exhibited photocurrent upon photoexcitation in the ultraviolet and visible wavelength range. Thermal and photostability of xylindein was also characterized, and it considerably exceeded that of conventional organic semiconductors such as pentacene derivatives.

Keywords: xylindein, fungi, Chlorociboria, pigment, hydrogen bonding, pH, carrier mobility, semiconductors

1. INTRODUCTION

Xylindein is one of a class of quinone pigments with a distinct blue-green hue. It is produced by fungi from the genus *Chlorociboria*. These wood-rot fungi are well-known in the forestry world for staining their host wood with a brilliant blue-green color, and xylindein-stained wood has been utilized in art since the fifteenth century, which attests to an extraordinary environmental stability of this pigment.[1] In 1965, Edwards and Kale[2] elucidated much of what is currently known about the structure and chemistry of xylindein, and their work was furthered by the efforts of Saikawa et al.[3] in 2000. However, the possibility of utilizing xylindein or other fungi-derived pigments in the context of organic electronics has heretofore not been explored, and (opto)electronic properties of such pigments have not been systematically characterized. Utilizing organic pigments such as xylindein for optoelectronic purposes promises a number of benefits, such as sustainability and reduced cost, potentially making both ecological and societal impact.[4] As such, we set out to investigate the fundamental photophysical and optoelectronic properties of xylindein and to lay foundations for similar studies of other fungi-derived pigments. Our particular goal is to establish the feasibility of optimizing these materials for sustainable organic electronics applications.

2. EXPERIMENTAL

2.1 Materials, sample preparation and measurement protocols

The structure of the xylindein molecule was confirmed by Saikawa et al.,[3] and it features a backbone of peri-xanthenoxanthene (PXX) as shown in Fig. 1(a). This structure gives xylindein the standardized IUPAC name of 8,16-Dihydroxy-3,11-dipropyl-3,4,11,12-tetrahydro-pyrano[4,3-h]pyrano[4',3';5,6]xantheno[2,1,9,8-klmna]xanthene-1,7,9,15-tetraone. Of interest here is that the structure of the molecule suggests the possibility of tuning two important effects that could impact xylindein optoelectronic and photophysical properties: hydrogen bonding (both intermolecular and intramolecular), and π-stacking between the adjacent PXX backbones of aromatic rings in the solid state. The xylindein used in our experiments was isolated from liquid culture of *C. aeruginosa*. *C. aeruginosa* (UAMH 11657) was cultured on 10 cm plates (2% malt, 1.5% agar in water) following the previously published procedures.[5] Mature fungal materials from 10 cm plates were transferred to 1 L liquid

Organic Photonic Materials and Devices XIX, edited by Christopher E. Tabor, François Kajzar, Toshikuni Kaino, Yasuhiro Koike, Proc. of SPIE Vol. 10101, 101010U · © 2017 SPIE
CCC code: 0277-786X/17/$18 · doi: 10.1117/12.2251265

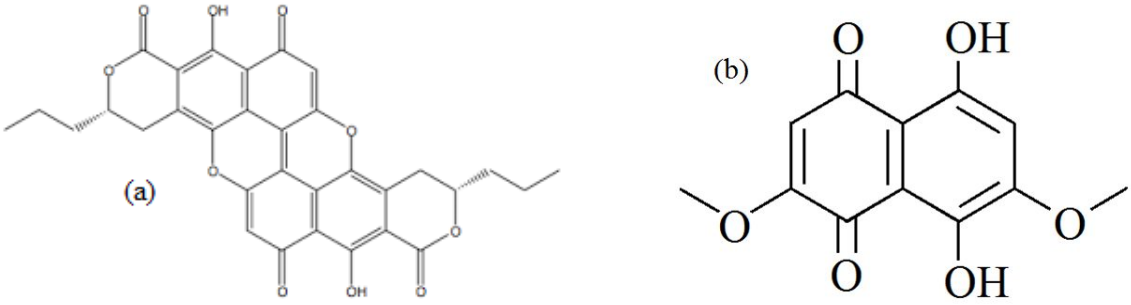

Figure 1. The molecular structures of (a) xylindein of *C. aeruginosa* and (b) red pigment of *S. cuboideum*.

batch bioreactors (2% malt in water) from which xylindein secreted into the liquid media was extracted and purified every 4-6 weeks.

Two other pigments derived from fungi were also examined for their optical properties. These two fungi species were *Scytalidium cuboideum*, which produces a vivid red color, and *Scytalidium ganodermophthorum*, characterized by a yellow-green hue. Molecular structure for the red pigment is shown in Fig. 1(b), whereas that for the yellow-green pigment is still being verified.

For measurements of optical absorption and photoluminescence (PL), we prepared 0.1 mM solutions of purified xylindein in several solvents of varying polarity and degree of interaction with polarized hydrogens (protic vs. aprotic). The solvents explored were chlorobenzene (CB), acetone (Ac), tetrahydrofuran (THF), isopropyl alcohol (IPA), and water. Due to low solubility of xylindein in water, the source of xylindein in aqueous solution used in our experiments was raw fungal culture of *Chlorociboria aeruginosa*. Additionally, this source enabled us to conduct pH-dependent measurements of optical properties. The xylindein in aqueous solution was added to various pH buffers calibrated to pH 7 (neutral), pH 10, and pH 13 using a pH meter. Absorption and PL measurements were taken on the resultant pH-varying xylindein solutions. Immediately subsequent to these measurements, the alkaline pH buffer solutions were brought back to pH 7 with a neutral buffer. To test the reversibility of pH-dependent changes, the absorption and PL measurements were then retaken on the "reversed" solutions.

Long-term photostability of xylindein solution was examined as follows. A small transparent vial of 10 μM xylindein in CB solution was prepared and left in a fume hood under constant exposure to visible light. Vials of 10 μM solutions of widely used organic semiconductors ADT-TES-F (a functionalized fluorinated anthradithiophene also known as diF TES ADT) and TIPS-Pentacene[6] were similarly prepared and left exposed to the visible light alongside the xylindein solution as benchmarks. Once a week at regular intervals, the photo-exposed solutions were removed and their absorption spectra measured. Such measurements continued for 7 months.

In the solid state, thermal stability of xylindein films was also tested. A film of xylindein was prepared on a glass slide by drop-casting a small volume of xylindein from CB solution. The resultant film was allowed to dry, and its absorption was then measured. Following this initial measurement, the film was then subjected to annealing on a hot plate for 20 minutes at a temperature of 50 °C (as measured by a thermocouple in thermal contact with the film) in air, after which the films absorption spectrum was measured again. The same process was repeated for an annealing temperature of 60 °C, and so on up to 210 °C. In each measurement, care was taken to ensure that the film was positioned identically so as to facilitate direct comparison of spectra across different annealing temperatures.

For measurements of (opto)electronic properties, 3 μL of 50 mM xylindein solution in CB was drop-cast onto coplanar or interdigitated Au/Cr electrodes with a 25 μm gap deposited on glass substrates.[7,8] This deposition method resulted in amorphous films as confirmed by the x-ray diffraction.

2.2 Measurements

Optical absorption and PL measurements were carried out using Ocean Optics USB2000, USB4000, or USB2000-FLG spectrometers as described in our previous publications.[7,9] For measurements of PL, excitation wavelengths of 355 nm, 532 nm, or 633 nm were utilized.

The current-voltage (I-V) characteristics from xylindein films were measured using Keithley 237 source-measure unit. The applied bias across the film was varied between 0 and 300 V in order to reach the transition between the linear and quadratic (space-charge-limited current (SCLC)) regime. The lower bound on charge carrier mobility was estimated using the thin-film approximation from the SCLC data as described in our previous publication.[10] For comparison, similar measurements were performed on a drop cast ADT-TES-F film[7] in a similar device structure. In order to probe photoresponse from xylindein films, the films were subjected to a steady applied bias voltage, and the change in the current under 633 nm, 532 nm, or 400 nm illumination was measured using Keithley 237.

3. RESULTS

In order to gain insight into optimized molecular structures and basic properties such as HOMO and LUMO energies, energies of excited states, transition dipole moments, etc. we performed DFT calculations for xylindein using Gaussian 09. To calibrate our calculations, we first calculated these properties for several molecules (including pentacene, functionalized anthradithiophene, and PXX) for which this information is available from the literature, both experimental and theoretical. For example, using the B3LYP 6-31G(d,p) basis set we obtained the HOMO-LUMO gap of 3.32 eV for an unsubstituted PXX, which compares well to 3.28 eV reported in the literature.[11] For a lowest excited singlet state (S1) energy, 2.73 eV (454 nm) was obtained for PXX, also comparable with the experimental literature values of 2.68-2.72 eV.[12] Xylindein of Fig. 1(a) yielded a considerably lower HOMO-LUMO gap (2.41 eV) and lower S1 energies (2.11 eV) as compared to the unsubstituted PXX. The red pigment of Fig. 1(b) was predicted to have a HOMO-LUMO gap of 2.85 eV.

As shown in Fig. 2, the lowest-energy optical transition observed in absorption spectra of xylindein (e.g. 660 nm, or 1.88 eV in CB solution) is considerably red-shifted with respect to theoretical predictions discussed above. Similar trend is observed in solutions of the red pigment of Fig. 1(b) (Fig. 3). Such red shift is most likely due to intermolecular hydrogen bonding (H-bonding) causing nanoaggregate formation, which is a well-known feature of H-bonded pigments.[13] The PL from solutions was weak, with PL quantum yields of below 1%, which could be due to intermolecular H-bonding, tautomerization reactions, or both.[13] While the absorption spectrum is not particularly sensitive to the solvent polarity, there is a pronounced (up to 50 nm) red shift of the spectrum in protic solvents as compared to aprotic ones (Fig. 2). This illustrates the importance of H-bonding in these materials, which was further explored by performing the pH-dependent measurements (Fig. 4). Similar spectra were obtained in the pH range between 7 and 10, whereas irreversible changes occurred at pH of 13. In this case, the 660 nm absorption band disappeared, whereas absorption in the UV region increased. These changes were accompanied by an almost three-fold increase in PL at 355 nm excitation, which suggests formation of emissive xylindein decomposition products in the in high-pH buffers.

Figure 5 shows results of the long-term photobleaching experiment on xylindein solution performed side-by-side with those of ADT-TES-F and TIPS-Pentacene. Here the spectra of the lowest-energy absorption bands (500-700 nm in xylindein and S0-S1 bands in ADT-TES-F and TIPS-Pentacene)[7] were integrated and normalized at the value at t = 0 (i.e. in a freshly prepared solution). Clearly, the photostability of xylindein is considerably superior not only to TIPS-Pentacene, but also to the ADT-TES-F whose excellent stability had enabled its utility as a fluorophore in single molecule fluorescence microscopy.[14]

Extraordinary stability also persists in films (Fig. 6), as no signs of degradation are apparent in the absorption spectra upon repeated film annealing in air up to temperatures of 180 °C, and complete degradation does not occur up to temperatures as high as 210 °C.

Finally, we tested (opto)electronic performance of xylindein films (Fig. 7). The effective carrier mobility estimated from the slopes of the current vs voltage-squared fits in the SCLC regime (bottom inset of Fig. 7) yielded values between 0.2 and 0.53 $cm^2/(V \cdot s)$, depending on the film, which compares well with those obtained in films of other H-bonded pigments.[6] Because the trap-free limit has not been reached in our experiments,

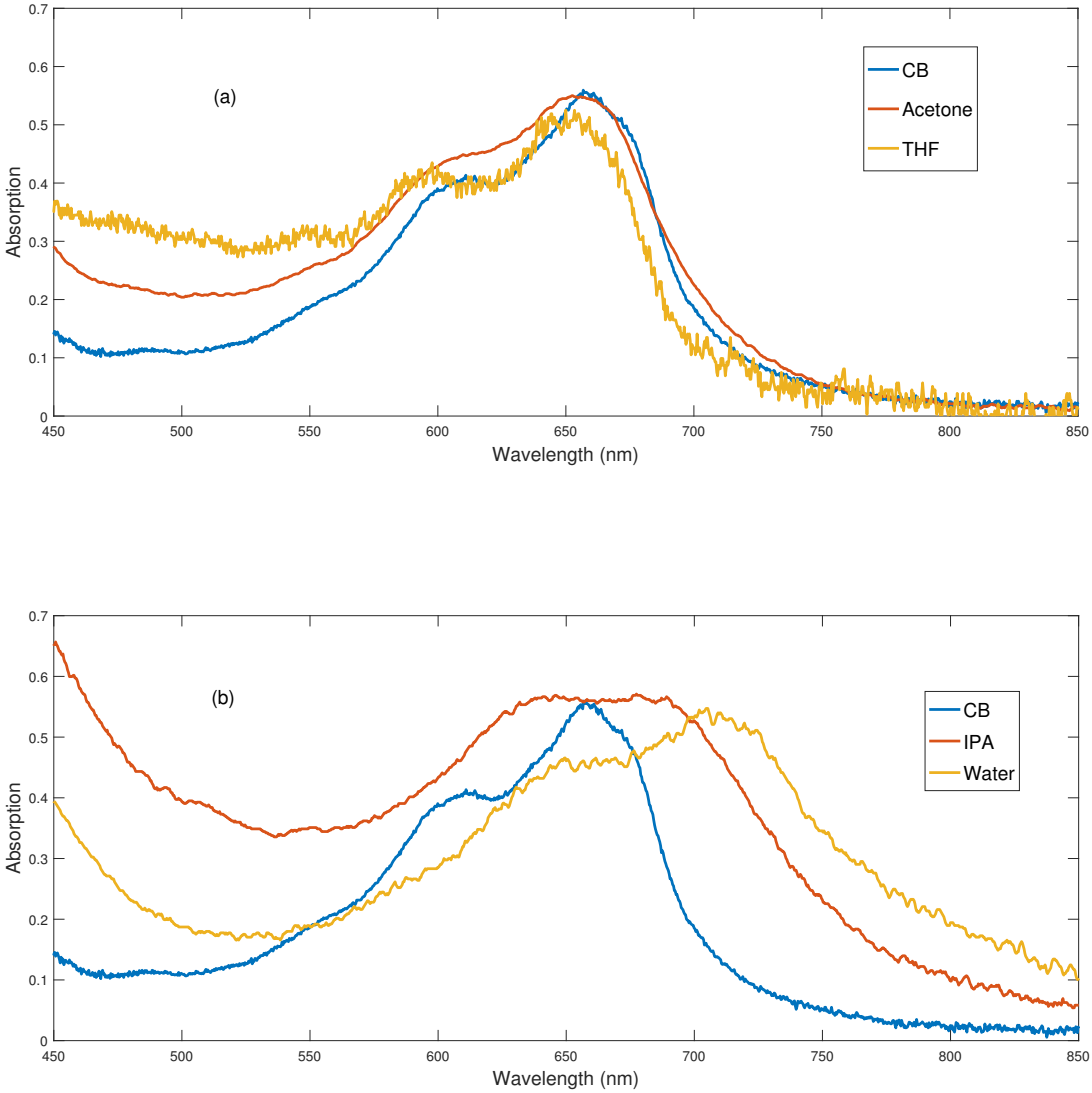

Figure 2. Optical absorption spectra of xylindein in (a) polar aprotic and (b) polar protic solvents compared against xylindein in nonpolar chlorobenzene.

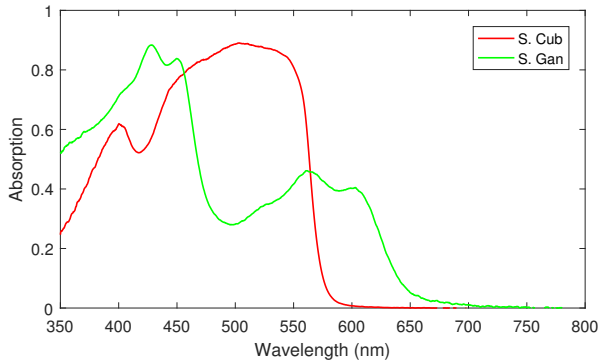

Figure 3. Optical absorption spectra obtained from solutions of red (*S.cub.*) and yellow-green (*S.Gan.*) fungi-derived pigments in dichloromethane.

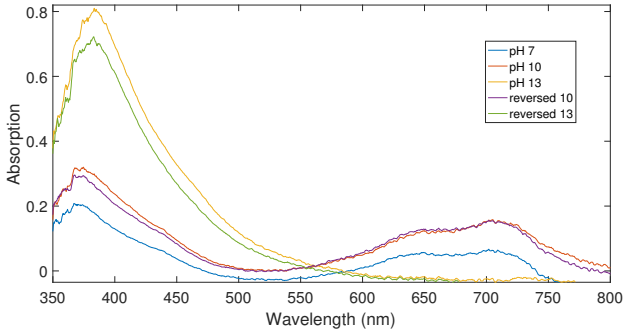

Figure 4. Optical absorption spectra of xylindein in aqueous neutral solution (pH 7) and several pH buffers. The data taken in solutions "reversed" to pH 7 after measurements in buffers with pH 10 and pH 13 are also included.

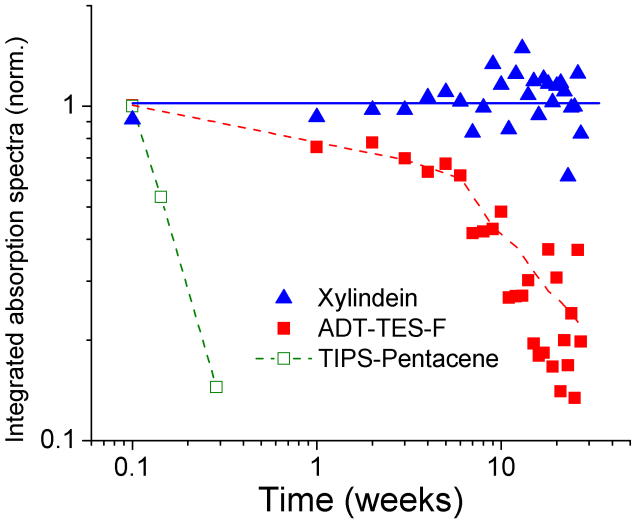

Figure 5. Photobleaching of xylindein in solution. Data for benchmark organic semiconductors ADT-TES-F and TIPS-Pentacene taken under the same conditions are also included. Lines provide a guide for the eye.

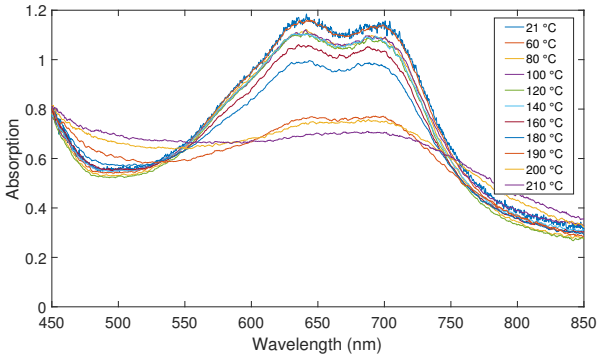

Figure 6. The absorption of xylindein film after having been annealed at successively higher temperatures in air.

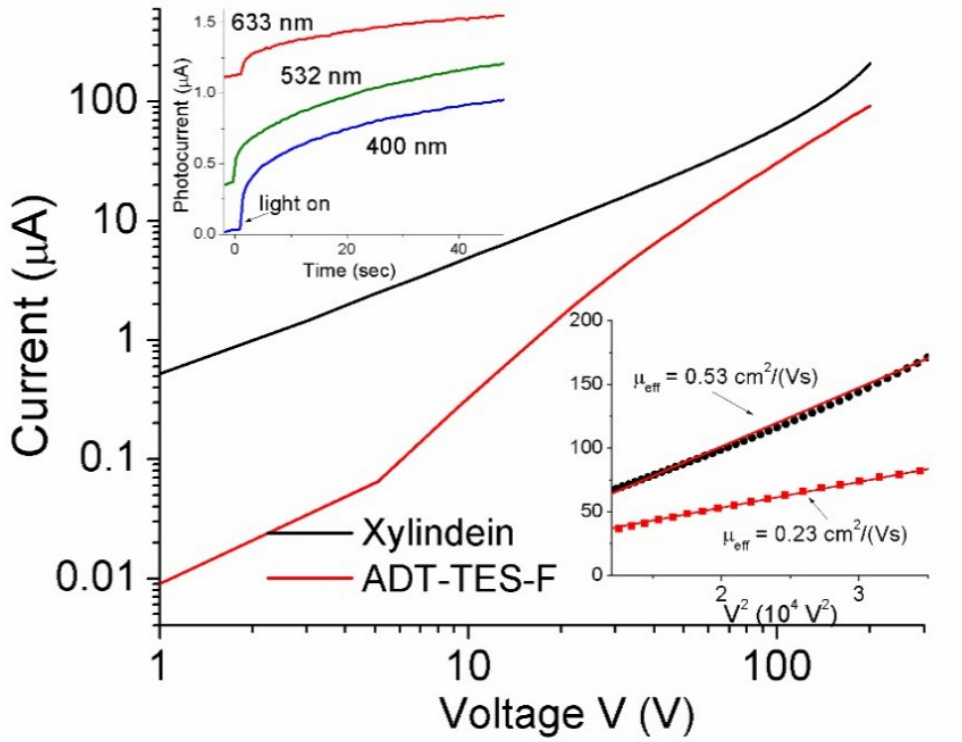

Figure 7. Current-voltage characteristics of xylindein amorphous film and ADT-TES-F polycrystalline film, both drop-cast under the same conditions on glass substrates with Au/Cr interdigitated electrodes. Inset on the bottom right shows currents in the SCLC regime, from which effective charge carrier mobility was estimated. Inset on the top left shows photoresponse (vertically offset for clarity) of the xylindein film to photoexcitation at wavelengths of 400 nm, 532 nm, and 633 nm.

the estimated effective mobility represents a lower bound, and the intrinsic value is likely considerably higher. Remarkably, these xylindein films are amorphous, in contrast to crystalline films of ADT-TES-F (data for which are also included in Fig. 7) or of H-bonded pigments such as indigo, Tyrian purple, epindolidione, or DPP derivatives with comparable mobilities.[15–17] Photoresponse was also observed from xylindein films upon 400 nm, 532 nm, and 633 nm excitation as shown in Fig. 7 (top inset).

4. CONCLUSION

Optical properties of fungi-derived pigments presented here are governed by an interplay of intermolecular and intramolecular H-bonding, the exact contribution of which into optical absorption and PL characteristics of pigments under study is yet to be determined. Photostability of xylindein in solution is considerably superior to that of benchmark organic semiconductor molecules. Additionally, xylindein films exhibit excellent thermal stability up to temperatures of at least 180 °C. Relatively high charge carrier mobilities of 0.2-0.5 $cm^2/(V \cdot s)$ were obtained in amorphous xylindein films and can potentially be improved in more ordered films. Xylindein and other fungi-derived pigments hold promise as a sustainable and low-cost source of extraordinarily stable organic electronic materials.

ACKNOWLEDGMENTS

We thank A. Fox and Prof. B. Gibbons for the x-ray diffraction measurements. This work was supported by the OSU General Research Fund (V. R. and O. O.) and via OSU URISC program (A. Q. and J. R.).

REFERENCES

[1] Robinson, S., Michaelson, H., and Robinson, J., [*Spalted Wood: The History, Science, and Art of a Unique Material*], Schiffer, Atglen, Pennsylvania (May 2016).

[2] Edwards, R. and Kale, N., "The structure of xylindein," *Tetrahedron* **21**, 2095–2107 (1965).

[3] Saikawa, Y., Watanabe, T., Hashimoto, K., and Nakata, M., "Absolute configuration and tautomeric structure of xylindein, a blue-green pigment of chlorociboria species," *Phytochemistry* **55**, 237–240 (2000).

[4] Głowacki, E., Voss, G., Leonat, L., Irimia-Vladu, M., Bauer, S., and Sariciftci, N., "Indigo and tyrian purple - from ancient natural dyes to modern organic semiconductors," *Israel Journal of Chemistry* **52**, 540–551 (2012).

[5] Weber, G., Chen, H., Hinsch, E., Freitas, S., and Robinson, S., "Pigments extracted from the wood-staining fungi chlorociboria aeruginosa, scytalidium cuboideum, and s. ganodermophthorum show potential for use as textile dyes,," *Coloration Technology* **130 (6)**, 445–452 (2014).

[6] Ostroverkhova, O., "Organic optoelectronic materials: Mechanisms and applications," *Chemical Reviews* **116**, 13279–13412 (2016).

[7] Platt, A., Day, J., Subramanian, S., Anthony, J. E., and Ostroverkhova, O., "Optical, fluorescent, and (photo)conductive properties of high-performance functionalized pentacene and anthradithiophene derivatives," *Journal of Physical Chemistry C* **113**, 14006–14014 (2009).

[8] Paudel, K., Johnson, B., Thieme, M., Haley, M., Payne, M., Anthony, J., and Ostroverkhova, O., "Enhanced charge photogeneration promoted by crystallinity in small-molecule donor-acceptor bulk heterojunctions," *Applied Physics Letters* **105**, 043301 (2014).

[9] Paudel, K., Johnson, B., Neunzert, A., Thieme, M., Purushothaman, B., Payne, M., Anthony, J., and Ostroverkhova, O., "Small-molecule bulk heterojunctions: Distinguishing between effects of energy offsets and molecular packing on optoelectronic properties," *J. Phys. Chem. C* **117 (47)**, 24752–24760 (2013).

[10] Day, J., Platt, A., Subramanian, S., Anthony, J., and Ostroverkhova, O., "Influence of organic semiconductor-metal interfaces on the photoresponse of functionalized anthradithiophene thin films," *J. Appl. Phys.* **105**, 103703 (2009).

[11] Wang, L., Duan, G., Ji, Y., and Zhang, H., "Electronic and charge transport properties of perixanthenoxanthene: The effects of heteroatoms and phenyl substitutions.," *J. Phys. Chem. C* **116 (43)**, 22679–22686 (2012).

[12] Lv, N., Xie, M., Gu, W., Ruan, H., and Qiu, S., "Synthesis, properties, and structures of functionalized peri-xanthenoxanthene," *Org. Lett* **15 (10)**, 2382–2385 (2013).

[13] Głowacki, E., Irimia-Vladu, M., Bauer, S., and Sariciftci, N., "Hydrogen-bonds in molecular solids - from biological systems to organic electronics," *J. Mater. Chem. B* **1**, 3742 (2013).

[14] Shepherd, W., Grollman, R., Robertson, A., Paudel, K., Hallani, R., Loth, M., Anthony, J., and Ostroverkhova, O., "Single-molecule imaging of organic semiconductors: Toward nanoscale insights into photophysics and molecular packing," *Chemical Physics Letters* **629**, 29–35 (2015).

[15] Głowacki, E., Romanazzi, G., Yumusak, C., Coskun, H., Monkowius, U., Voss, G., Burian, M., Lechner, R., Demitri, N., and G. Redhammer, e. a., "Epindolidiones-versatile and stable hydrogen-bonded pigments for organic field-effect transistors and light-emitting diodes," *Adv. Funct. Mater.* **25**, 776–787 (2015).

[16] Głowacki, E., Coskun, H., Blood-Forsythe, M., Monkowius, U., Leonat, L., Grzybowski, M., D. Gryko, D., White, M., Aspuru-Guzik, A., and Sariciftci, N., "Hydrogen-bonded diketopyrrolopyrrole (dpp) pigments as organic semiconductors," *Org. Electron.* **15 (12)**, 3521–3528 (2014).

[17] Sytnyk, M., Daniel, E., Yakunin, S., Voss, G., Scho, W., Kriegner, D., Stangl, J., Trotta, R., Gollner, C., and S. Tollabimazraehno, e. a., "Hydrogen-bonded organic semiconductor micro- and nanocrystals: From colloidal syntheses to (opto-)electronic devices," *J. Am. Chem. Soc.* **136 (47)**, 16522–16533 (2014).